Available online at www.sciencedirect.com
SCIENCE DIRECT®
ELSEVIER
Journal of Computational and Applied Mathematics 168 (2004) 245–254
JOURNAL OF COMPUTATIONAL AND APPLIED MATHEMATICS
www.elsevier.com/locate/cam

Adaptive multigrid and domain decomposition methods in the computation of electromagnetic fields☆

R.H.W. Hoppe

Institute of Mathematics, University of Augsburg, Universitätsstraße 14, Augsburg D-86159, Germany

Received 14 August 2002; received in revised form 15 May 2003

Abstract

We consider efficient and robust adaptive multigrid and domain decomposition methods for the computation of electromagnetic fields in the low-frequency regime, i.e., for the quasistationary limit of Maxwell's equations based on curl-conforming edge element discretizations. Emphasis is on hybrid smoothing and nonmatching grids (mortar edge elements) as well as on adaptive grid refinement relying on residual type a posteriori error estimation. Numerical results are given to illustrate the performance of the multigrid solvers and the a posteriori error estimators. As a technologically relevant problem, we briefly address the computation of eddy currents in converter modules used as electric drives for high-power electromotors.

MSC: 65M50; 65M55; 65M60; 78A25; 78A55

Keywords: Electromagnetic field computation; Multigrid methods; Domain decomposition; Edge elements; A posteriori error estimation

1. Introduction

The use of standard nodal finite elements in the numerical solution of Maxwell's equations is marred by the occurrence of spurious modes causing severe stability problems, if no proper gauging is performed. Moreover, in case of corner or edge singularitites there might be solutions that due to a lack of regularity cannot be approximated by nodal finite elements at all. On the other hand, it is well-known that curl-conforming edge elements [17] avoid such difficulties, since they

☆ This work has been supported by the Federal Ministry for Education and Research (BMBF) under Grants No. 03HO7AU1, No. 03HOM3A1 and by the German National Science Foundation (DFG) under Grant No. HO877/4-2.
E-mail address: hoppe@math.uni-augsburg.de (R.H.W. Hoppe).

0377-0427/$ - see front matter
doi:10.1016/j.cam.2003.05.023

are much closer to the variational formulation of boundary and initial-boundary value problems in electromagnetics (see, for instance [5,6]).

In particular, we deal with multigrid algorithms whose basic ingredients are hybrid or distributive smoothing processes that take care of the nontrivial kernel of the discrete curl-operator. The characteristic feature is an additional defect correction on the subspace of irrotational vector fields [1,9,11]. Adaptive grid refinement/coarsening can be performed by means of efficient and reliable a posteriori error estimators. We present a residual estimator based on an appropriate Helmholtz decomposition [2].

For nonoverlapping, geometrically conforming partitions of the computational domain we further consider a domain decomposition approach featuring edge element discretizations of the subdomain problems with respect to individual triangulations of the subdomains that do not necessarily match on the interfaces. Such techniques require to impose weak continuity constraints on the interfaces that can be taken care of by appropriately chosen Lagrange multipliers. We give an outline of such mortar edge element methods with emphasis on the proper construction of multiplier spaces on the skeleton of the decomposition as well as on the efficient solution of the resulting discrete saddle point problem [3,10,12,18].

The performance of the adaptive solution techniques will be illustrated by a variety of numerical results. As a technological application, we consider the modeling and simulation of converter modules in high power electronics (cf., e.g., [14–16]).

2. Adaptive multigrid methods

We consider electromagnetic field problems in the low-frequency regime that can be adequately described by the quasistationary limit of Maxwell's equations also known as the eddy current equations

$$\sigma \frac{\partial \mathbf{E}}{\partial t} + \mathbf{curl}\, \mu^{-1}\, \mathbf{curl}\, \mathbf{E} = -\frac{\partial \mathbf{J}_I}{\partial t}, \tag{1}$$

where $\mathbf{E}$ is the electric field, $\mathbf{J}_I$ stands for an intrinsic current density, σ is the conductivity, and μ refers to the magnetic permeability.

If we discretize implicitly in time, e.g., by the backward Euler scheme, we are led to an elliptic boundary value problem for the double curl-operator

$$\mathbf{curl}\, \alpha\, \mathbf{curl}\, \mathbf{E} + \beta \mathbf{E} = \mathbf{f} \tag{2}$$

with appropriate boundary conditions on the boundary of the computational domain $\Omega \subset \mathbb{R}^3$ which we assume to be a bounded polyhedral domain with boundary $\Gamma = \partial\Omega$. We denote by $L^2(\Omega)$ and $L^2(\Gamma)$ the Hilbert spaces of square integrable functions on Ω and Γ with inner products $(\cdot,\cdot)_{0,D}$ and norms $\|\cdot\|_{0,D}$, $D = \Omega$ or $D = \Gamma$ and refer to $H^r(\Omega)$ and $H^s(\Gamma)$, $r, s \in \mathbb{R}$, as the Sobolev spaces with norms $\|\cdot\|_{r,\Omega}$ and $\|\cdot\|_{s,\Gamma}$, respectively. For vector fields we further set $\mathbf{H}^r(\Omega) := (H^r(\Omega))^3$, $\mathbf{H}^s(\Gamma) := (H^s(\Gamma))^3$, $\mathbf{H}(\mathbf{curl};\Omega) := \{\mathbf{q} \in \mathbf{L}^2(\Omega) \,|\, \mathbf{curl}\, \mathbf{q} \in \mathbf{L}^2(\Omega)\}$ with norm $\|\mathbf{q}\|_{\mathrm{curl},\Omega} := (\|\mathbf{q}\|^2_{0,\Omega} + \|\mathbf{curl}\, \mathbf{q}\|^2_{0,\Omega})^{1/2}$, and $\mathbf{H}(\mathrm{div};\Omega) := \{\mathbf{q} \in \mathbf{L}^2(\Omega) \,|\, \mathrm{div}\, \mathbf{q} \in L^2(\Omega)\}$ with norm $\|\mathbf{q}\|_{\mathrm{div},\Omega} := (\|\mathbf{q}\|^2_{0,\Omega} + \|\mathrm{div}\, \mathbf{q}\|^2_{0,\Omega})^{1/2}$. Finally, we denote by $\mathbf{H}_0(\mathbf{curl};\Omega)$ the subspace $\mathbf{H}_0(\mathbf{curl};\Omega) := \{\mathbf{q} \in \mathbf{H}(\mathbf{curl};\Omega) \,|\, \mathbf{n} \wedge \mathbf{q} = \mathbf{0} \text{ on } \Gamma\}$ of vector fields with vanishing tangential trace on Γ and by $\mathbf{H}^0(\mathbf{curl};\Omega)$ the subspace $\mathbf{H}^0(\mathbf{curl};\Omega) :=$

$\{\mathbf{q} \in \mathbf{H}(\mathbf{curl}; \Omega) \,|\, \mathbf{curl}\, \mathbf{q} = \mathbf{0}\}$ of irrotational vector fields. We set $\mathbf{H}_0^0(\mathbf{curl}; \Omega) := \mathbf{H}_0(\mathbf{curl}; \Omega) \cap \mathbf{H}^0(\mathbf{curl}; \Omega)$.

The variational formulation of (1) is then given by:

find $\mathbf{j} \in \mathbf{H}_0(\mathbf{curl}; \Omega)$ such that

$$a(\mathbf{j}, \mathbf{q}) = \ell(\mathbf{q}), \quad \mathbf{q} \in \mathbf{H}_0(\mathbf{curl}; \Omega), \tag{3}$$

where

$$a(\mathbf{j}, \mathbf{q}) := \int_\Omega (\alpha\, \mathbf{curl}\, \mathbf{j} \cdot \mathbf{curl}\, \mathbf{q} + \beta\, \mathbf{j} \cdot \mathbf{q})\, \mathrm{d}\mathbf{x}, \quad \ell(\mathbf{q}) := \int_\Omega \mathbf{f} \cdot \mathbf{q}\, \mathrm{d}\mathbf{x}.$$

Given a hierarchy of simplicial triangulations T_k, $0 \leqslant k \leqslant \ell$, of the computational domain $\Omega \subset \mathbb{R}^3$, for $D \subset \Omega$ we denote by $N_k(D)$, $E_k(D)$, and $F_k(D)$ the sets of vertices, edges, and faces of T_k in D and by $P_i(D)$ resp. $\tilde{P}_i(D)$ the set of polynomials resp. homogeneous polynomials of degree $i \in \mathbb{N}_0$ on D. For $T \in T_k$, Nédélec's lowest order curl-conforming edge element is given by $\mathbf{Nd}_1(T) := (P_0(T))^3 + \mathbf{S}_1(T)$, where $\mathbf{S}_1(T) := \{\mathbf{q} \in (\tilde{P}_1(T))^3 \,|\, \mathbf{q}(\mathbf{x}) \cdot \mathbf{x} = 0,\ \mathbf{x} \in T\}$. Note that any $\mathbf{q} \in \mathbf{Nd}_1(T)$, $T \in T_k$ is uniquely determined by the degrees of freedom $\int_E \mathbf{t}_E \cdot \mathbf{q}\, \mathrm{d}s$, $E \in E_k(T)$, where $\mathbf{t}_E$ is the tangential unit vector with respect to the edge $E \in E_k(T)$ (cf., e.g., [17]). For later use in Section 3, we further denote by $\mathbf{RT}_0(T) := (P_0(T))^3 + \mathbf{x}P_0(T)$ the lowest order Raviart–Thomas element with the degrees of freedom given by $\int_E \mathbf{n}_E \cdot \mathbf{q}\, \mathrm{d}s$, $E \in E_k(T)$, where $\mathbf{n}_E$ is the exterior unit normal vector with respect to the edge $E \in E_k(T)$ (cf., e.g., [8]).

We refer to $\mathbf{Nd}_1(\Omega; T_k) := \{\mathbf{q} \in H(\mathbf{curl}; \Omega) \,|\, \mathbf{q}|_T \in \mathbf{Nd}_1(T),\ T \in T_k\}$ as the associated lowest order $\mathbf{H}(\mathbf{curl})$-conforming edge element spaces and to $\mathbf{RT}_0(\Omega; T_k) := \{\mathbf{q} \in H(\mathrm{div}; \Omega) \,|\, \mathbf{q}|_T \in \mathbf{RT}_0(T),\ T \in T_k\}$ as the associated lowest order $\mathbf{H}(\mathrm{div})$-conforming Raviart–Thomas spaces. Then, the edge element discretized problem on the finest grid ℓ reads as follows:

Find $\mathbf{j}_\ell \in \mathbf{Nd}_{1,0}(\Omega; T_\ell) := \{\mathbf{q}_\ell \in \mathbf{Nd}_1(\Omega; T_\ell) \,|\, \mathbf{n} \wedge \mathbf{q}_\ell = 0 \text{ on } \Gamma\}$ such that

$$a(\mathbf{j}_\ell, \mathbf{q}_\ell) = \ell(\mathbf{q}_\ell), \quad \mathbf{q}_\ell \in \mathbf{Nd}_{1,0}(\Omega; T_\ell). \tag{4}$$

The multigrid solution of (4) has to take into account the nontrivial kernel $\mathbf{Nd}_{1,0}^0(\Omega; T_k) := \{\mathbf{q}_k \in \mathbf{Nd}_{1,0}(\Omega; T_k) \,|\, \mathbf{curl}\, \mathbf{q}_k = 0\}$ of the discrete curl-operator which is given by $\mathbf{Nd}_{1,0}^0(\Omega; T_k) = \mathbf{grad}\, S_{1,0}(\Omega; T_k)$, where $S_{1,0}(\Omega; T_k)$ is the standard FE-space of continuous, piecewise linear finite elements.

In particular, it requires a hybrid smoother on all levels $1 \leqslant k \leqslant \ell$ that can also be used as an iterative solver on the lowest level $k = 0$. Given an iterate $\mathbf{j}_k$ on level k, the hybrid smoother consists of $\kappa > 0$ Gauss–Seidel sweeps applied to (4) resulting in $\bar{\mathbf{j}}_k$ followed by a defect correction on $\mathbf{Nd}_{1,0}^0(\Omega; T_k) = \mathbf{grad}\, S_{1,0}(\Omega; T_k)$: Perform $\kappa > 0$ Gauss–Seidel iterations on

$$\int_\Omega \beta\, \mathbf{grad}\, u_k \cdot \mathbf{grad}\, v_k\, \mathrm{d}\mathbf{x} = r(\mathbf{grad}\, v_k), \quad v_k \in S_{1,0}(\Omega; T_k),$$

where $r(\cdot)$ stands for the residual with respect to $\bar{\mathbf{j}}_k$

$$r(\mathbf{grad}\, v_k) := \ell(\mathbf{grad}\, v_k) - a(\bar{\mathbf{j}}_k, \mathbf{grad}\, v_k), \quad v_k \in S_{1,0}(\Omega; T_k)$$

and $u_k^{(0)} = 0$ is used as a startiterate.

The intergrid transfers (prolongations, restrictions) can be chosen canonically (cf. [1,9]). Grid- and level-independent multigrid convergence has been established in Ref. [9].

A residual-based error estimator in the energy norm $|||\mathbf{j}|||^2 := (\alpha, \mathbf{curl}\,\mathbf{j}, \mathbf{curl}\,\mathbf{j})_{0,\Omega} + (\beta\,\mathbf{j}, \mathbf{j})_{0,\Omega}$ can be derived using the Helmholtz-type decomposition $\mathbf{H}_0(\mathbf{curl}; \Omega) = \mathbf{H}_0^0(\mathbf{curl}; \Omega) \oplus \mathbf{H}_0^{\perp}(\mathbf{curl}; \Omega)$, where $\mathbf{H}_0^{\perp}(\mathbf{curl}; \Omega)$ is the orthogonal complement of $\mathbf{H}_0^0(\mathbf{curl}; \Omega)$ with respect to the L^2-inner product $(\beta\cdot, \cdot)_{0,\Omega}$ and thus represents a subspace of weakly solenoidal vector fields.

If we split the error $\mathbf{e}_\ell := \mathbf{j} - \mathbf{j}_\ell$ according to $\mathbf{e}_\ell = \mathbf{e}_\ell^0 + \mathbf{e}_\ell^{\perp}$, where $\mathbf{e}_\ell^0 \in \mathbf{H}_0^0(\mathbf{curl}; \Omega)$ and $\mathbf{e}_\ell^{\perp} \in \mathbf{H}_0^{\perp}(\mathbf{curl}; \Omega)$, we find that $\mathbf{e}_\ell^0$ and $\mathbf{e}_\ell^{\perp}$ satisfy

$$(\beta\,\mathbf{e}_\ell^0, \mathbf{q}^0)_{0,\Omega} = r(\mathbf{q}), \quad \mathbf{q}^0 \in \mathbf{H}_0^0(\mathbf{curl}; \Omega),$$

$$(\alpha\,\mathbf{curl}\,\mathbf{e}_\ell^{\perp}, \mathbf{curl}\,\mathbf{q}^{\perp})_{0,\Omega} + (\beta\,\mathbf{e}_\ell^{\perp}, \mathbf{q}^{\perp})_{0,\Omega} = r(\mathbf{q}), \quad \mathbf{q}^{\perp} \in \mathbf{H}_0^{\perp}(\mathbf{curl}; \Omega).$$

The advantage of the Helmholtz decomposition is that the irrotational and weakly solenoidal part of the error can be estimated separately [2]. In particular, under some technical assumption it can be shown that there exist constants $\gamma_1, \gamma_2 > 0$ and $\Gamma_1, \Gamma_2 > 0$, depending only on Ω, α, β, and on the local geometry of T_ℓ such that

$$\gamma_1 \delta^{(1)} - \gamma_2 \delta^{(2)} \leqslant |||\mathbf{e}_\ell||| \leqslant \Gamma_1 \delta^{(1)} + \Gamma_2 \delta^{(2)}. \tag{5}$$

Here, $\delta^{(1)}, \delta^{(2)}$ refer to the error terms

$$\delta^{(1)} := \sum_{v=0}^{1} \left[\left(\sum_{T \in T_\ell} (\delta_T^{(v)})^2 \right)^{1/2} + \left(\sum_{F \in F_h(\Omega)} (\delta_F^{(v)})^2 \right)^{1/2} \right], \quad \delta^{(2)} := \left(\sum_{T \in T_\ell} (\delta_T^{(2)})^2 \right)^{1/2}$$

with the local contributions $\delta_T^{(v)}$, $0 \leqslant v \leqslant 2$, and $\delta_F^{(v)}$, $0 \leqslant v \leqslant 1$ given by

$$\delta_T^{(0)} := h_T \|\mathrm{div}(\beta^{1/2}\mathbf{j}_\ell)\|_{0,T},$$

$$\delta_T^{(1)} := h_T \|\alpha^{-1/2}(\mathbf{f}_\ell - \mathbf{curl}\,\alpha\,\mathbf{curl}\,\mathbf{j}_\ell - \beta\,\mathbf{j}_\ell)\|_{0,T},$$

$$\delta_T^{(2)} := h_T \|\alpha^{-1/2}(\mathbf{f} - \mathbf{f}_\ell)\|_{0,T},$$

$$\delta_F^{(0)} := h_F^{1/2} \|\beta_A^{-1/2}[\mathbf{n} \cdot \beta\mathbf{j}_\ell]_J\|_{0,F},$$

$$\delta_F^{(1)} := h_F^{1/2} \|\alpha_A^{-1/2}[\mathbf{n} \wedge \alpha\,\mathbf{curl}\,\mathbf{j}_\ell]_J\|_{0,F}.$$

Note that $h_T := \mathrm{diam}\,T$, $h_F := \mathrm{diam}\,F$, $\mathbf{f}_\ell$ is the L^2-projection of $\mathbf{f}$ onto $\prod_{T \in T_h} (P_1(T))^3$, α_A, β_A are the arithmetic averages of α, β on F, and $[\mathbf{n}\cdot\beta\,\mathbf{j}_\ell]_J$, $[\mathbf{n}\wedge\alpha\,\mathbf{curl}\,\mathbf{j}_\ell]_J$ refer to the jumps of $\mathbf{n}\cdot\beta\mathbf{j}_\ell$, $\mathbf{n}\wedge\alpha\,\mathbf{curl}\,\mathbf{j}_\ell$ across F.

3. Domain decomposition on nonmatching grids

We consider a nonoverlapping decomposition of Ω into n mutually disjoint subdomains

$$\bar{\Omega} = \bigcup_{i=1}^{n} \Omega_i, \quad \Omega_i \cap \Omega_j \neq \emptyset, \quad 1 \leqslant i \neq j \leqslant n. \tag{6}$$

We assume the decomposition to be geometrically conforming, i.e., two adjacent subdomains either share a face, an edge, or a vertex. We use individual simplicial triangulations T_i of the subdomains

$\Omega_i,\ 1 \leqslant i \leqslant n$, regardless the situation on the skeleton of the decomposition

$$S := \bigcup_{i \neq j} \Gamma_{ij}, \quad \Gamma_{ij} := \bar{\Omega}_i \cap \bar{\Omega}_j \neq \emptyset, \tag{7}$$

consisting of the interfaces Γ_{ij} between adjacent subdomains Ω_i and Ω_j where typically nonconforming nodal points will arise. The interfaces Γ_{ij} inherit two different triangulations, namely T_{ij} from the triangulation T_i of Ω_i and T_{ji} from the triangulation T_j of Ω_j. We denote by Ω_j the mortar and by Ω_i the nonmortar side.

We refer to $Nd_{1,0}(\Omega_i; T_i), 1 \leqslant i \leqslant n$, as the corresponding edge element spaces with vanishing tangential traces on Γ and consider the product space

$$V_h := \prod_{i=1}^{n} Nd_{1,0}(\Omega_i; T_i) \tag{8}$$

with norm $\|\cdot\|_V := (\sum_{i=1}^{n} \|\cdot\|^2_{\mathrm{curl};\Omega_i})^{1/2}$.

Due to the occurrence of nonconforming edges on the interfaces between adjacent subdomains, there is a lack of continuity across the interfaces: neither the tangential traces $\boldsymbol{n} \wedge \mathbf{q_h}$ nor the tangential trace components $\boldsymbol{n} \wedge (\boldsymbol{n} \wedge \mathbf{q_h})$ can be expected to be continuous. We denote by $\mathbf{Nd}_1(\Gamma_{ij}; T_{ij})$ resp. $\mathbf{RT_0}(\Gamma_{ij}; T_{ij})$ the edge element space resp. the lowest order Raviart–Thomas space on Γ_{ij} with respect to the triangulation T_{ij} inherited from the nonmortar side. We note that $(\boldsymbol{n} \wedge \mathbf{q_h})|_{\Gamma_{ij}} \in \mathbf{RT_0}(\Gamma_{ij}; T_{ij})$ resp. $(\boldsymbol{n} \wedge (\boldsymbol{n} \wedge \mathbf{q_h}))|_{\Gamma_{ij}} \in \mathbf{Nd_1}(\Gamma_{ij}; T_{ij})$. Therefore, continuity can be enforced either in terms of the tangential traces or the tangential trace components. If we choose the tangential traces, the multiplier space $\mathbf{M_h(S)}$ can be constructed according to

$$\mathbf{M_h(S)} := \prod_{\Gamma_{ij} \subset S} \mathbf{M_h}(\Gamma_{ij}) \tag{9}$$

with $\mathbf{M_h}(\Gamma_{ij})$ chosen such that

$$\mathbf{RT_{0,0}}(\Gamma_{ij}; T_{ij}) \subset \mathbf{M_h}(\Gamma_{ij}), \quad \dim \mathbf{M_h}(\Gamma_{ij}) = \dim \mathbf{RT_{0,0}}(\Gamma_{ij}; T_{ij}).$$

$\mathbf{M_h(S)}$ is equipped with a mesh-dependent norm $\|\cdot\|_{\mathbf{M_h(S)}}$ (cf., e.g., [10]; see [3,18] for alternative approaches).

The mortar edge element approximation of (2) then requires the solution of the saddle point problem:

Find $(\mathbf{j_h}, \boldsymbol{\lambda_h}) \in \mathbf{V_h} \times \mathbf{M_h(S)}$ such that

$$a_h(\mathbf{j_h}, \mathbf{q_h}) + b_h(\mathbf{q_h}, \boldsymbol{\lambda_h}) = \int_\Omega \mathbf{f} \cdot \mathbf{q_h}, \quad \mathbf{q_h} \in \mathbf{V_h}, \tag{10}$$

$$b_h(\mathbf{j_h}, \boldsymbol{\mu_h}) = 0, \quad \boldsymbol{\mu_h} \in \mathbf{M_h(S)}, \tag{11}$$

where the bilinear forms $a_h(\cdot,\cdot) : \mathbf{V_h} \times \mathbf{V_h} \to \mathbf{R}$ and $b_h(\cdot,\cdot) : \mathbf{V_h} \times \mathbf{M_h(S)} \to \mathbf{R}$ are given by

$$a_h(\mathbf{j_h}, \mathbf{q_h}) := \sum_{i=1}^{n} \int_{\Omega_i} (\alpha\, \mathbf{curl}\, \mathbf{j_h} \cdot \mathbf{curl}\, \mathbf{q_h} + \beta\, \mathbf{j_h} \cdot \mathbf{q_h})\, \mathrm{d}x, \quad \mathbf{j_h}, \mathbf{q_h} \in \mathbf{V_h},$$

$$b_h(\mathbf{q_h}, \boldsymbol{\mu_h}) := \sum_{\Gamma_{ij} \subset S} \int_{\Gamma_{ij}} [\boldsymbol{n} \wedge \mathbf{q_h}]_J \cdot \boldsymbol{\mu_h}\, \mathrm{d}\sigma, \quad \mathbf{q_h} \in \mathbf{V_h}, \quad \boldsymbol{\mu_h} \in \mathbf{M_h(S)}.$$

Denoting by $B_h : \mathbf{V_h} \to \mathbf{M_h(S)}^*$ the operator associated with $b_h(\cdot,\cdot)$, it can be shown that the bilinear form $a_h(\cdot,\cdot)$is elliptic on $\operatorname{Ker} B_h$, and the bilinear form $b_h(\cdot,\cdot)$ satisfies the LBB-condition

$$\inf_{\boldsymbol{\mu}_\mathbf{h}\in\mathbf{M_h(S)}} \sup_{\mathbf{q_h}\in\mathbf{V_h}} \frac{b_h(\mathbf{q_h},\boldsymbol{\mu}_\mathbf{h})}{\|\mathbf{q_h}\|_{\mathbf{V_h}}\|\boldsymbol{\mu}_\mathbf{h}\|_{\mathbf{M_h(S)}}} \geqslant \beta > 0. \tag{12}$$

The numerical solution of the resulting algebraic saddle point problem has to take into account the nontrivial kernel of the discrete curl-operator which is subdomain-wise given by the subspace of irrotational vector fields spanned by the gradients of the finite element functions in $S_{1,0}(\Omega_i; T_i), 1 \leqslant i \leqslant n$. In the framework of domain decomposition methods on nonmatching grids, we may adopt the multigrid method outlined in Section 2. However, we must observe that the defect correction has to be performed with regard to mortar Lagrange finite element techniques along the lines of [4,7,13]. In particular, the hybrid smoothing process consists of the following steps:

Step 1 (*Smoothing on the edge element discretized problem*):

$$\begin{pmatrix} \mathbf{j}_h^{\nu+1} \\ \boldsymbol{\lambda}_\mathbf{h}^{\nu+1} \end{pmatrix} = \begin{pmatrix} \mathbf{j}_h^{\nu} \\ \boldsymbol{\lambda}_\mathbf{h}^{\nu} \end{pmatrix} - \begin{pmatrix} R_1 & B_1^{\mathrm{T}} \\ B_1 & 0 \end{pmatrix}^{-1} \left\{ \begin{pmatrix} A_1 & B_1^{\mathrm{T}} \\ B_1 & 0 \end{pmatrix} \begin{pmatrix} \mathbf{j}_h^{\nu} \\ \boldsymbol{\lambda}_\mathbf{h}^{\nu} \end{pmatrix} - \begin{pmatrix} \mathbf{b} \\ \mathbf{0} \end{pmatrix} \right\},$$

where $R_1 := \operatorname{diag}(R_1^{(1)},\ldots,R_1^{(n)})$ with $R_1^{(i)}, 1 \leqslant i \leqslant n$, being Gauss–Seidel sweeps on the subdomain problems

$$\int_{\Omega_i} (\alpha\, \mathbf{curl}\, \mathbf{j_h} \cdot \mathbf{curl}\, \mathbf{q_h} + \beta\, \mathbf{j_h} \cdot \mathbf{q_h})\, \mathrm{d}x = \int_{\Omega_i} \mathbf{f} \cdot \mathbf{q_h}\, \mathrm{d}x, \quad \mathbf{q_h} \in Nd_{1,0}(\Omega_i; T_i).$$

Step 2 (*Defect correction on the irrotational part*):

$$\begin{pmatrix} \varphi_h^{\nu+1} \\ \eta_h^{\nu+1} \end{pmatrix} = \begin{pmatrix} \varphi_h^{\nu} \\ \eta_h^{\nu} \end{pmatrix} - \begin{pmatrix} R_2 & B_2^{\mathrm{T}} \\ B_2 & 0 \end{pmatrix}^{-1} \left\{ \begin{pmatrix} A_2 & B_2^{\mathrm{T}} \\ B_2 & 0 \end{pmatrix} \begin{pmatrix} \varphi_h^{\nu} \\ \eta_h^{\nu} \end{pmatrix} - \begin{pmatrix} r \\ 0 \end{pmatrix} \right\},$$

where $R_2 := \operatorname{diag}(R_2^{(1)},\ldots,R_2^{(n)})$ with $R_2^{(i)}, 1 \leqslant i \leqslant n$, being Gauss–Seidel sweeps on

$$\int_{\Omega_i} \beta\, \mathbf{grad}\, \varphi_h \cdot \mathbf{grad}\, v_h\, \mathrm{d}x = r(v_h), \quad v_h \in S_{1,0}(\Omega_i; T_i),$$

the right-hand side representing the residual

$$r(v_h) := \int_{\Omega_i} \mathbf{f} \cdot \mathbf{grad}\, v_h\, \mathrm{d}x - a_h|_{\Omega_i}(\mathbf{j}_h, \mathbf{grad}\, v_h).$$

Step 3 (*Additive correction*): Denoting by $\mathbf{j}_h$ and φ_h the results of the smoothing steps 1 and 2, we finally compute

$$\mathbf{j}_h^{\mathrm{new}} := \mathbf{j}_h + \mathbf{grad}\, \varphi_h.$$

Note that in both Steps 1 and 2 we use a nondiagonal preconditioner only for the unknowns associated with edges resp. grid points in the interior of the subdomains, but a diagonal preconditioner on the skeleton.

For a residual-type a posteriori error estimator in the framework of mortar edge elements we refer to [11,12].

4. Numerical results

For an illustration of the performance of the multigrid solver with hybrid smoothing, we have to considered the eddy currents equation (2) with $\alpha = 1$ and different values of β for a smooth solution on $\Omega = (-1,+1)^3$ and in case of a corner/edge singularity for $\Omega = (-1,+1)^3 \backslash ([0,1]^2 \times [-1,+1])$.

Tables 1 and 2 display the convergence rates of multigrid V-cycles with one pre- and one post-smoothing step on levels $1 \leqslant \ell \leqslant 6$ with $h_\ell = 2^{-(\ell+1)}$.

We see typical grid- and level-independent convergence rates that clearly demonstrate the efficiency as well as the robustness of the multigrid approach.

We have also computed the effectivity indices, i.e., the ratio of the estimated and the true error, for the residual-based error estimator presented in Section 2. In case $\alpha = 1$ and $\Omega = (-1,+1)^3$, Tables 3 and 4 contain the effectivity indices for a wide range of β-values in case of a weakly solenoidal solution ($\mathbf{j} = \mathbf{curl}\ (\sin(\pi yz), \cos(\pi xz), \sin(\pi xy))$) and an irrotational solution ($\mathbf{j} = \mathbf{grad}\ (xyz)$).

The effectivity indices reflect both the efficiency and reliability of the residual a posteriori error estimator (for further results see [2]).

As an industrially relevant application of the mortar edge element method described in Section 3, we consider the computation of eddy currents in DC–AC converter modules that are based on the pulse width modulation technique and used as electric drives for high power electromotors.

As shown in Fig. 1, such a converter module consists of semiconductor devices (Insulated Gate Bipolar Transistors (IGBTs) and Gate Turn-Off Thyristors (GTOs)) serving as valves for the electric currents. The IGBTs and GTOs are connected to each other and linked to the power source and the load by copper-made bus bars (cf. Fig. 1 (left)). The interconnecting bus bars are of a complex 3D geometrical structure displaying several contacts where the semiconductor devices can be attached (cf. Fig. 1 (right)).

Due to steep current ramps (several kA) and fast switching times (< 100 ns), eddy currents are generated in the bus bars that can be computed by means of the potential formulation of the eddy currents equations in terms of a scalar electric potential φ and a magnetic vector potential $\mathbf{A}$

$$\operatorname{div}(\sigma\, \mathbf{grad}\, \varphi) = 0 \quad \text{in } \Omega, \tag{13}$$

$$\boldsymbol{n} \cdot \sigma\, \mathbf{grad}\, \varphi = \begin{cases} -I_v(t) & \text{on } \Gamma_v, \\ 0 & \text{on } \Gamma \setminus \Gamma_v, \end{cases} \tag{14}$$

$$\sigma \frac{\partial \mathbf{A}}{\partial t} + \mathbf{curl}\, \mu\, \mathbf{curl}\, \mathbf{A} = \begin{cases} -\sigma\, \mathbf{grad}\, \varphi & \text{in } \Omega, \\ 0 & \text{in } \mathbf{R}^3 \setminus \bar{\Omega}, \end{cases} \tag{15}$$

the latter one with appropriate initial and boundary conditions.

Here, I_v are the fluxes associated with the contacts Γ_v satisfying $\sum_{v=1}^{N} I_v = 0$. Note that the potential formulation (13)–(15) can be derived from Maxwell's equations by a quasistationary approximation based on a separation of the time scales and a decoupling of the potentials by means of the Coulomb gauge. For a single bus bar, we have used a domain decomposition into two

Table 1
Convergence rates (smooth solution)

ℓ	2	3	4	5	6
$\beta = 0.1$	0.15	0.16	0.16	0.16	0.16
$\beta = 0.5$	0.15	0.16	0.16	0.16	0.16
$\beta = 1.0$	0.15	0.16	0.16	0.16	0.16
$\beta = 2.0$	0.15	0.16	0.16	0.16	0.16
$\beta = 10.0$	0.14	0.16	0.16	0.16	0.16

Table 2
Convergence rates (singularity)

ℓ	2	3	4	5	6
$\beta = 0.1$	0.18	0.19	0.20	0.21	0.22
$\beta = 0.5$	0.18	0.19	0.20	0.21	0.22
$\beta = 1.0$	0.18	0.19	0.21	0.21	0.22
$\beta = 2.0$	0.17	0.19	0.21	0.21	0.22
$\beta = 10.0$	0.16	0.19	0.20	0.22	0.22

Table 3
Effectivity indices (weakly solenoidal sol.)

ℓ	0	1	2	3	4
$\beta = 10^{-4}$	5.26	5.94	7.07	7.51	7.72
$\beta = 10^{-2}$	5.25	6.23	7.08	7.50	7.71
$\beta = 1.00$	3.82	6.08	6.92	7.34	7.55
$\beta = 10^{+2}$	1.86	3.14	3.99	4.46	4.96
$\beta = 10^{+4}$	1.70	3.17	3.98	4.34	4.49

Table 4
Effectivity indices (irrotational sol.)

ℓ	0	1	2	3	4
$\beta = 10^{-4}$	4.21	4.70	4.90	4.98	5.01
$\beta = 10^{-2}$	4.21	4.70	4.90	4.98	5.01
$\beta = 1.00$	4.21	4.70	4.89	4.98	5.01
$\beta = 10^{+2}$	4.22	4.68	4.87	4.96	5.01
$\beta = 10^{+4}$	4.22	4.66	4.84	4.92	4.96

subdomains (interior/exterior) and discretized (15) implicitly in time by the backward Euler scheme while using nonconforming P1 elements for (13), (14) and lowest order Nédélec elements for (15) with respect to adaptively generated hierarchies of simplicial triangulations for the two subdomains that do not match on the interface.

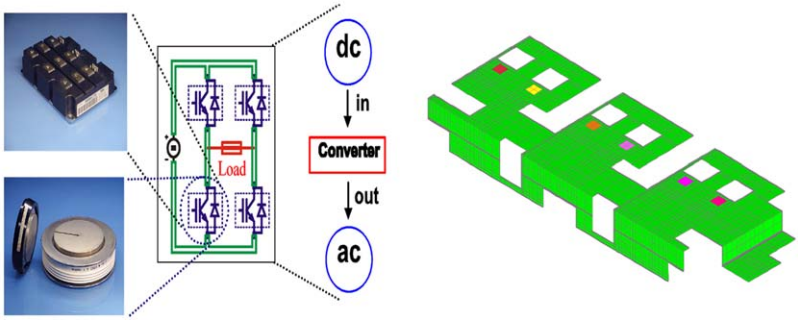

Fig. 1. Converter module (left) and bus bar (right).

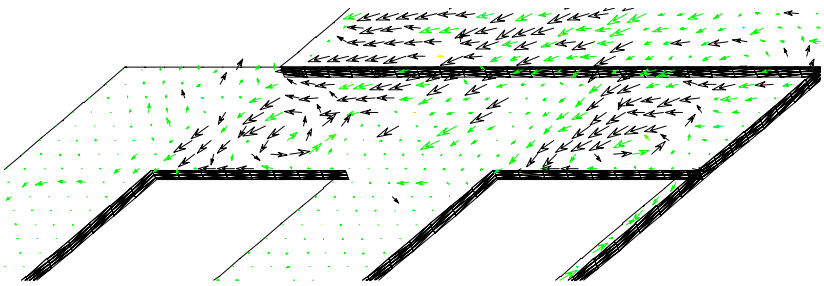

Fig. 2. Distribution of the magnetic induction between two ports (zoom).

Fig. 2 displays a visualization of the distribution of the magnetic induction ($\mathbf{B} = \mathbf{curl}\,\mathbf{A}$) in the vicinity of two ports.

For further results and an optimal design of AC–DC converter modules by topology optimization we refer to [14–16].

References

[1] R. Beck, P. Deuflhard, R. Hiptmair, R.H.W. Hoppe, B. Wohlmuth, Adaptive multilevel methods for edge element discretizations of Maxwell's equations, Surveys Math. Ind. 8 (1999) 271–312.

[2] R. Beck, R. Hiptmair, R.H.W. Hoppe, B. Wohlmuth, Residual based a posteriori error estimators for eddy current computation, Math. Modelling Numer. Anal. 34 (2000) 159–182.

[3] F. BenBelgacem, A. Buffa, Y. Maday, The mortar finite element method for 3D Maxwell equations: first results, Report 99023, Laboratoire d'Analyse Numérique, Université Pierre et Marie Curie, Paris, 1999.

[4] F. BenBelgacem, Y. Maday, The mortar element method for three dimensional finite elements, Math. Modelling Numer. Anal. 31 (1997) 289–302.

[5] D. Boffi, F. Brezzi, L. Gastaldi, Mixed finite elements for Maxwell's eigenproblem: the question of spurious modes, in: H.G. Bock, et al., (Eds.), Proceedings of the Second European Conference on Numerical Mathematics and Advanced Applications, Heidelberg, Germany, September 28–October 3, 1997, World Scientific, Singapore, 1998, pp. 180–187.

[6] A. Bossavit, Computational Electromagnetism. Variational Formulation, Complementarity, Edge Elements, Academic Press, San Diego, CA, 1998.

[7] D. Braess, W. Dahmen, Stability estimates of the mortar finite element method for 3-dimensional problems, East–West J. Numer. Math. 6 (1998) 249–264.
[8] F. Brezzi, M. Fortin, Mixed and Hybrid Finite Element Methods, Springer, Berlin, Heidelberg, New York, 1991.
[9] R. Hiptmair, Multigrid method for Maxwell's equations, SIAM J. Numer. Anal. 36 (1999) 204–225.
[10] R.H.W. Hoppe, Mortar edge elements in R^3, East–West J. Numer. Anal. 7 (1999) 159–173.
[11] R.H.W. Hoppe, Efficient numerical solution techniques in electromagnetic field computation, in: Proceedings of the Conference of ECCM 2001, Cracow, Poland, June 26–29, 2001 (CD-ROM).
[12] R.H.W. Hoppe, Adaptive domain decomposition techniques in electromagnetic field computation and electro-thermomechanical coupling problems, in: F. Brezzi, et al. (Eds.), Proceedings of the Fourth European Conference on Numer. Math. and Advanced Applications, Ischia, Italy, July 23–27, 2001, Springer, Milan, 2003, pp. 201–218.
[13] R.H.W. Hoppe, Y. Iliash, Y. Kuznetsov, Y. Vassilevski, B. Wohlmuth, Analysis and parallel implementation of adaptive mortar element methods, East–West J. Numer. Math. 6 (1998) 223–248.
[14] R.H.W. Hoppe, S. Petrova, V. Schulz, Topology optimization of high power electronic devices, in: K.H. Hoffmann, et al., (Eds.), Proceedings of the Oberwolfach Conference Optimale Steuerung komplexer dynamischer Strukturen, June 4–10, Oberwolfach, Germany, International Series of Numerical Mathematics, Vol. 139, Birkhäuser, Basel, 2002, pp. 119–131.
[15] R.H.W. Hoppe, S. Petrova, V. Schulz, 3D structural optimization in electromagnetics, in: M. Garbey, et al., (Eds.), Proceedings of the 13th International Conference on Domain Decomposition Methods and Applications, Lyon, October 9–12, 2000, 2002.
[16] R.H.W. Hoppe, S. Petrova, V. Schulz, A primal-dual Newton-type interior-point method for topology optimization, J. Optim. Theory Appl. 114 (2002) 545–571.
[17] J. Nédélec, Mixed finite elements in R^3, Numer. Math. 35 (1980) 315–341.
[18] F. Rapetti, Approximation des equations de la magnetodynamique en domaine tournant par la méthode des elements avec joints, Ph.D. Thesis, Université Pierre et Marie Curie, Paris, 2000.